JETIR.ORG ISSN: 2349-5162 | ESTD Year : 2014 | Monthly Issue
JOURNAL OF EMERGING TECHNOLOGIES AND INNOVATIVE RESEARCH (JETIR)
An International Scholarly Open Access, Peer-reviewed, Refereed Journal

Doping Behaviour of Ag and Sb Metallic Impurities in Chalcogenide Glasses

Satya Prakash Singh
Associate Professor
Department of Physics, Christ Church College, Kanpur, India
satya1209prakash@gmail.com

Abstract: **It is well known that the semiconducting materials, particularly semiconducting thin films, have significant physical and chemical properties which are often sharply improved by combining them in different proportions for making their alloys (or) compounds. A wide range of photoinduced phenomena exhibited by chalcogenide glasses make them suitable for a variety of optical applications, such as in the correction of spatial uniformity of filters or the fabrication of integrated optical components and devices like selective optical filters, couplers and modulators, and planar waveguides for soliton Kerr propagation for ultrafast optical application. This review is based on Ag and Sb doped chalcogenide thin films and their subsequent effect on various properties of the host matrix due to alteration in structure, bonding etc. The developments of these metal-doped thin films and their physicochemical aspects were also discussed.**

Index Terms - Density of defect states (DOS), Photoluminescence (PL), Optical band gap (E_g)

I. INTRODUCTION

Exploration of new materials with improved, tunable linear and nonlinear optical property is of great interest in photonic device fabrication. Chalcogenide (CG)-based thin films are the most famously known candidates for their wide applications in photonics and device applications over the range of 0.6 μm to 15 μm. Their wide range of applications for passive devices like lenses, windows, optical fibers, etc., and active devices like laser fibers, nonlinear devices, etc., makes them more attractive. In CGs, the photoinduced effect is very influential due to the impact of the localized state present in the middle of the bandwidth gap. These photo-doped metal CG films were useful in the application of holographic recording. The change in thickness of the metal-doped CG material due to photo induction is insignificant. For high-speed optical communication, nonlinearity is considered to be the key ingredient. But the nonlinearity demonstrated by silica glass is small, so to be used for switching and communicational application, either long device length or a more excellent power supply are required. Thus, materials with high nonlinearity are necessary to produce nonlinear photonic circuits with low threshold and condensing. CG materials are highly nonlinear and offered for switching in telecommunication applications [1]. CG materials possess nonlinear susceptibility, two orders of magnitude higher than silica. These nonlinear properties become active when they are influenced by a strong electric field. This nonlinearity demonstrated by CG is greatly affected by the doping effect resulting from the subsequent change in the material system.

CGs, when irradiated by electromagnetic radiation in the visible range (i.e., white light), then they experience numerous modifications in their electrical and photo-electrical properties. The alteration in such properties is probably linked with the formation of two kinds of defect centres: (i) charged (D^+ and D^-) centres, and (ii) neutral (D^0) centres. The characteristic feature of CGs is the occurrence of localized energy levels in the mobility gap because of the non-appearance of ordered structuring in addition to numerous intrinsic structural defects. In CGs, the experiment of electrical conductivity in the dark and light conditions is a significant approach to acquire valuable evidence concerning the formation of defect centres. Such studies are also useful for searching their suitable applications because this kind of experiment examines the applicability of a specific material for solar panels and other optoelectronic applications.

Analysis of optical absorption spectra is one of the most productive tools for understanding and developing the band structure and energy gap of both crystalline and amorphous non-metallic material. The optical absorption edges are described using the non-direct transmission model proposed by Tauc and the optical energy gaps are calculated by Tauc's extrapolation. Optical energy gap is formally defined as the intercept of the plot of $(\alpha h\nu)^{0.5}$ against $(h\nu)$. The high absorption region determines the optical energy gap. The strong absorption region, involves optical transition between valence and conduction band. The absorption coefficient of amorphous semiconductor in the high-absorption region ($\alpha = 10^4 cm^{-1}$) can be calculated by using the Tauc's relation [2]

$$\alpha h\nu = B\left(h\nu - E_g \right)^m \quad (1)$$

where B is a constant, E_g is the optical energy gap of the material and m determines the type of transition (m = ½ for the direct transition and m = 2 for indirect allowed transition).

The doping of impurity silver atom (Ag) into CG systems causes variations in their properties by increasing their network connectivity structure, enhancing their chemical and thermal stability, and increasing the electrical conductivity of the system[3][4]. Also, silver is a more reflective and soluble metal in CG alloys. It easily forms bonds with defect levels present in CG alloys, which helps to improve its optical and electrical properties. Excellent crystallization speed and significant resistance contrast were also observed in the thin Ag embedded CG layers [5]. Apart from tuning the optoelectronic properties, the incorporation of several metals leads to tailoring the properties of the host CG materials by changing their internal glass network connectivity, internal structure, and bonding [6]. These changes in the CG glass matrix, therefore, alter the average number of coordination and bring structural changes such as rigid to intermediate to flexible and vice versa in the vitreous network. Therefore, such behaviour adjusts the physioptical properties accordingly in a controlled trend concerning industry and technology requirements [7]. Apart from thechange in the network connectivity, some metals such as antimony (Sb) can create new defects in the network with substitution and affect the short and medium-range order in the glass network, also used as a chemical modifier resulting in several characteristic modifications. Sb can unpin Fermi level and supports carrier-type reversal, from p to n, helping to expand the glassy region of the network, enhance thermal stability, and increment in IR transmission, therefore reshaping the chemical composition structures by considering the perspective of device fabrication [8]. This review summarizes the doping impact of Ag and Sb metallic impurities on the structural, electrical and optical behaviour of different CG glasses.

II. METAL DOPING IN CHALCOGENIDE GLASSES

The addition of different elements into the CG glasses in order to modify their optoelectronic properties was popular even from the late 60s. The addition of metals to the CG system contributes primarily to the formation of cross-linked structures and enhances other physical properties.

A. Silver doped chalcogenide glasses

Silver-chalcogenide glasses have potential applications in the fields of chemistry, optoelectronics, biology, and optics and have attracted much interest in glass science and technology either for their potential applications in holographic recording and photolithography, or as fast-ion-conducting glasses, in solid-state batteries. In the silver (Ag) -based system, Ag is assumed to be a glass former. Incorporating Ag in the CG material enhances the electrical conductivity of Ag alloys by crossing over the CG chains and making the system stable. In glasses with high concentrations of Ag (>15%), the electrical conductivity is governed by the Ag^+ ionic conduction, while for small percentages of Ag (x<5), hole conductivity is dominated [9]. Different ways of preparation were reported in which silver is added either during the preparation of the amorphous alloys [10-12] or with the photodissolution technique [9,13,14].

Due to the ionic character, the introduction of Ag results in different structural alterations in the materials, which in turn modifies the band structure and hence the electrical properties of the material. For example, the increase in Ag concentration doping in the Ge–S system (x =57.1 at. %) enhances the conductivity of the order of 22 times of the doping concentration (x = 30 at. %) Ag in the same system [15].This enhancement of conductivity is due to the ionic character of Ag^+ ions. It has been reported that increasing the concentration of Ag in CG glasses, i.e., from 5 at. % of Ag to 30 at. % of the same system modifies from ionic conductor [15-16] to superionic conductor system [17]. Mytilineou et al.[18] have studied the optical and electrical properties of amorphous selenium(a-Se), and amorphous selenium containing silver, a-$Se_{100-x}Ag_x$, with x<5 or silver iodine, $Se_{100-x}(AgI)_x$ and $Se_{100-2x}Ag_xI_x$, with x≤15, in order to determine the influence of each additive on the density of defect states(DOS) in a-Se. The studies reveal that the addition of Ag or of AgI does not induce any impurity bands in the gap of a-Se and that the higher percentages of Ag kill the photoconductivity of a-Se. The addition of Ag or AgI to a-Se decreases the optical gap by 0.1eV with the

addition of 5 at. % Ag or with 15 at.% AgI into the a-Se matrix. Ag is introduced as three or four fold-coordinated element and cross-links the Se chains, while the iodine (I) acts as a chain terminator [12]. The energy of the Ag 4d bands lies near the top of the valance band formed by the lone pairs of the Se atoms. The two bands interact forming d-p bonding states in the upper valence region. This energy band picture could cause the observed decrease of the optical gap of a-Se with the addition of Ag or AgI [14]. The spectral dependence of the photoconductivity shows a peak at 2.4 eV, which is attributed to band-to-band optical transitions.

The dc conductivity measurements at high electric fields in vacuum evaporated thin films of amorphous $Se_{80-x}Te_{20}Ag_x$ (x=0, 5, 10, 15) have been reported by Singh et al. [19]. The current-voltage (I-V) characteristics have been measured at various fixed temperatures. At low electric fields, an ohmic behaviour is observed. However, at high electric fields (E~10^4V/cm), non- ohmic behaviour is observed. An analysis of the experimental data confirms the presence of space charge limited conduction (SCLC) in all the glassy materials. Using the theory of SCLC, the density of defect states (DOS) near the Fermi level is calculated; it does not change significantly with increasing concentration of Ag in the pure binary $Se_{80}Te_{20}$ system. Linear plots of ln I/V vs. V give different curves (slopes) for different values of electrode spacing d which confirms the SCLC mechanism in studied glassy samples.

Ag-doped As_2Se_3 glasses were prepared by the melt-quenching method and the influence of silver doping on the glass structure and optical properties was studied using Raman and UV-Vis-IR spectroscopy and differential scanning calorimetry by Zha et al. [20]. It was reported that for Ag concentrations less than 15 at.%, introduction of Ag into As_2Se_3 glasses mainly leads to the formation of Ag-Se covalent bonds, resulting in destruction of the glass network. This manifests itself by a decrease in the glass transition temperature and low frequency shifts in the As-Se Raman band. When the Ag concentration was higher than 25 at%, some Ag atoms exist in the glass matrix as coordinative bonds, resulting in a slight increase in the glass transition temperature and high frequency shifts in the Raman peaks.

Effect of impurity addition of Ag, Bi and Ge on the optical properties of vacuum evaporated thin films of $Se_{80}Te_{20}$, $(Se_{80}Te_{20})_{98}M_2$ have been reported by Mainika et al. [21], using transmission spectra. The spectral distribution function curve of transmittance for the composition $Se_{80}Te_{20}$, $(Se_{80}Te_{20})_{98}Ag_2$, $(Se_{80}Te_{20})_{98}Bi_2$ and $(Se_{80}Te_{20})_{98}Ge_2$ films have been used to compute refractive and absorption indices, using the Swanepoel method [22]. Optical transmission spectra of these thin films are shown in Figure 1. Figure 2 shows a linear relation of $(\alpha h\nu)^{0.5}$ versus $(h\nu)$, which indicates that the absorption mechanism in this system is non-transition. The values of optical energy gap (E_g) obtained for indirect allowed transition for investigated thin films of $Se_{80}Te_{20}$ and $(Se_{80}Te_{20})_{98}Ag_2$ by making $(\alpha h\nu)^{0.5}$ 0 are 1.41 and 1.43 resp. An increase in E_g for Ag based system was explained with electronegativity (χ) difference between Se-Te and Se-Te-Ag alloy, calculated using Sanderson's principle [23]. According to this principle, χ of the alloy is the geometric mean of χ of the constituent elements and the probability of defects formation will be more when the χ difference is large. According to Mulliken [24], the χ is the average of the ionization potential and the electron affinity. Since it is difficult to assign an electron affinity value for a semiconducting alloy therefore, it will be appropriate to correlate the χ with optical energy gap. χ of Se-Te-Ag is 2.44 which is less than the χ of Se-Te (2.46), so that the optical energy gap increases with decreasing χ.

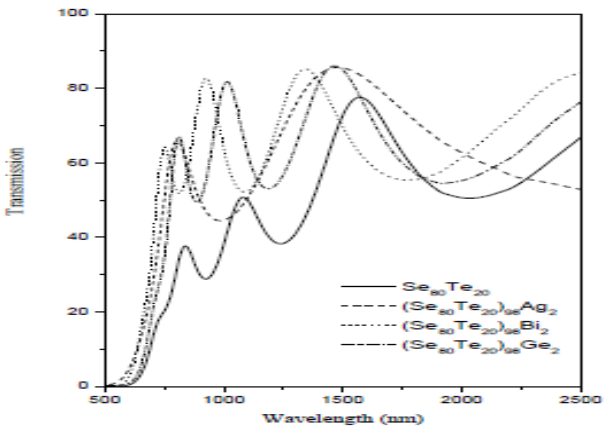

Figure1:Transmission spectra of $Se_{80}Te_{20}$, $(Se_{80}Te_{20})_{98}M_2$ (M = Ag, Bi, Ge) thin films.[21]

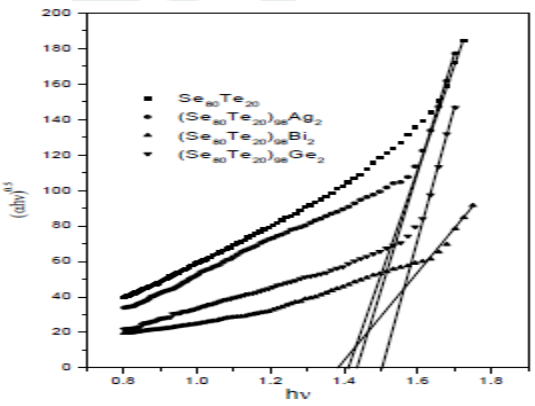

Figure 2: Plot of $(\alpha h\nu)^{0.5}$ versus $(h\nu)$ for $Se_{80}Te_{20}$, $(Se_{80}Te_{20})_{98}M_2$ (M = Ag, Bi, Ge) thin films.[21]

DC electrical conductivity (σ_{DC}) measurement by four probe system at room temperature (293K) of $(GeTe_4)_{100-x}Ag_x$ (x=0, 5, 10, 15, and 20) and $(GeTe_4)_{100-x}(AgI)_x$ (x=0, 5, 10, 12.5, 15, 17.5, 20, and 25) glasses prepared by melt-quenching method have been reported by Cui et al [25]. σ_{DC} shows a monotonic increase for $(GeTe_4)_{100-x}Ag_x$ glasses from 6.37×10^{-6} S·cm $^{-1}$ up to 9.22×10^{-5} S·cm^{-1} when Ag is increased from 0% up to 20%. The band gap is a major factor determining the electronic (or hole) conductivity of a semiconductor. For $(GeTe_4)_{100-x}Ag_x$ glasses, it was found

that by adding Ag, optical band gap was firstly decreased from 0.645eV (x = 0) down to 0.573eV (x = 15) and then remains constant which was attributed to the structural transformation. Ag enters the glass structure and forms its own connected structure [26]. In this constrained network structure, Ag may cause an increase in disorder and induce energy levels in the band gap. Due to the high doping concentration, the density of states of these dopants increases and forms a continuum of states just like in the bands and effectively decreases the band gap. This behavior contributes to the migration of photo-generated electrons. As a result, more electrons can go to conduction band, generating a higher conductivity. When Ag content is beyond 15%, the intermediate levels in the band gap are fully occupied and the glass becomes more metallic. Thus, the glass optical band gap stops decreasing. However, the electrons of Ag still enter into the glass network continuously, generating a higher conductivity. By adding Ag, the $(GeTe_4)_{100-x}Ag_x$ glasses always exhibit an electronic-type conductivity that monotonously increases.

Messaddeq et al. [27] reported the compositional effect of Ag on the optical and structural properties of $As_{40}S_{60}$ ChG thin films. $Ag_X(As_{40}S_{60})_{100-X}$ thin films (x = 7, 15, 25, 50) were deposited on glass slides by a co-evaporation technique under vacuum. Photoinduced birefringence (PIB; an optical characteristic exhibited by amorphous solids under special circumstances, originating from structural anisotropy) was induced using light provided from a continuous argon-ion laser operating at 488 nm. The thin films structural changes after irradiation were characterized by Raman spectroscopy which indicates that addition of Ag induces the breaking of sulfur ring units and favors the creation of Ag-S-Ag bridging bonds. The study reveals the dependence between PIB and silver amount showing that an increased photoinduced birefringence in the As-S-Ag thin film could be attributed to As_4S_4 molecules formed during the process. The ability to induce optical birefringence in an amorphous ChG material provides a pathway to control the photoinduced polarization of light and could have a significant impact on the conception of optical elements. Optical transmission spectra shows a shift of the bandgap position and the optical band gap decreases from 2.38 eV to 1.72 eV when the Ag amount is increased from 0 to 50 at.%. This red shift of the absorption edge is probably caused by the formation of additional defect states localized just above the valence band, coming from the atomic substitution of As by Ag [28].

Luminescent Ag-doped $Zn_xCd_{1-x}S$ semiconductor films have been synthesized by Chen et al. [29] *via* a facile and green method in the open air at 260 °C using precursors. $NH_3{\cdot}H_2O$ (28–30%) were used as solvent, and 3-mercaptopropionic acid was used as the capping agents. As-prepared quantum dot thin films exhibit a tunable emission covering the whole visible light region. It was reported that the photoluminescence (PL) properties of Ag doped $Zn_xCd_{1-x}S$ quantum dot thin films were strongly influenced by Ag doping content, sintering temperature, and time. The PL peak changes from 559 nm to 572 nm with an increase in Ag content from 0.1% to 0.5%. For 1.0% Ag, the observed PL intensity showed a maximum value. PL intensity shifted with sintering temperature due to the increase of particle size with an increase in reaction temperature. The absolute PL quantum yields reached as high as 24.6%, which have a high potential application in luminescent, transparent, and conductive thin films.

The effect of Ag addition on linear and non-linear optical properties of thermally evaporated $(Ge_2Sb_2Te_5)_{100-x}Ag_x$(x = 0, 1, 3 and 10) thin films (thickness ~700 nm) from single transmission spectra was studied by Singh et al [30]. The decrease in measured optical parameters up to 3% Ag doping is due to a decrease in the density of localized states (DOS) in the mobility gap. Ag doping in the $(Ge_2Sb_2Te_5)_{100-x}Ag_x$ system mainly influences the nonlinearity by decreasing the nonlinear susceptibility up to *x* = 3 at. % and then increases due to the distortion in the host matrix because of the high concentration of Ag. This variation is mainly caused by the phase change between amorphous and crystalline, which allows the system to customize several properties. The interpretation of χ and nonlinear optical susceptibility with Ag content at 1500 nm wavelength showed a decreasing trend with doping concentration up to 3 at.%; after that, it starts increasing due to distortion in the host matrix at higher doping concentration. The conductivity increases with the increase in the energy of incident light due to the excitation of thin film electrons. With Ag addition in $Ge_2Sb_2Te_5$ (GST) up to 3%, optical conductivity decreases, and 10% Ag doping optical conductivity increases.

Kumar et al. [31] reported the role of Ag additives on light induced metastable defects in Se–In glassy alloys using thermally stimulated current (TSC) technique. Measurements were made in the amorphous thin films of $Se_{90}In_{10-x}Ag_x$(x = 0, 2, 4, 8) prior to and after exposing to white light for different exposure times (0–1.5 hrs). The density of light induced metastable defects increases with exposure time, and the fractional increase in light induced metastable defect density decreases as Ag concentration increases indicating their suitability in processing and applications with optoelectronic devices. A microscopic model of Shimakawa [32] has been used to explain the generation of light-induced metastable defects and in terms of valence alternation pairs (VAPs). Yakoubi et al. [33] synthesized Ag-doped $Cd_xZn_{1-x}S$ quantum dots (QDs) in aqueous solution and investigated the effects of the Ag^+ doping concentration and of the Cd/Zn ratio on the structural and optical properties of the dots. PL emission of Core Ag:$Cd_xZn_{1-x}S$ QDs can be tuned from 478 to 610nm by varying the dopant concentration or the composition of the $Cd_xZn_{1-x}S$ host material. The highest PL quantum yield (25%) is obtained when using 2 or 3.5% doping in Ag^+. The PL quantum yield increased substantially (44%) after capping the Ag:$Cd_xZn_{1-x}S$ core with a ZnS shell.

Ag:$Cd_xZn_{1-x}S$ QDs are of high potential as nanophosphors or as fluorescent probes for bio-imaging due to long excited-state lifetimes (1–2 μs) and high photostability.

Defect states also enhance the nonlinear opticals of the system. This behaviour was reported by Viswanathan et al. [34] in the Ag-doped Ge–Se–Sb system. Ag concentration in Ge–Se–Sb film improves the nonlinear absorptions that ultimately form the mid-gap states known as the localized defect states. A clear red shift in the transmission spectra and an increase in the amplitude of the interference fringes in the Ge–Se–Sb–Ag films inevitably cause an increase in the refractive index. High value of refractive index and high glass transition temperature observed in GeSeSbAg sample as compared with GeSeSb glasses are attributed to the difference in bonding statistics of these glasses.

Guerrero et al. [35] deposited Silver doped cadmium sulphide (CdS:Ag) thin films on a polyethylene terephthalate (PET) flexible substrate through the chemical bath deposition method by varying the silver deposition time. XRD shows an evolution from the original hexagonal CdS pattern to the appearance of characteristic signals of metallic Ag. The absorbance study in the visible range between 430 and 800 nm shows that the addition of Ag doping at different deposition times caused the absorption to increase and absorption edge shifts to the longer wavelength region. The absorption edge at 537 nm at deposition time of 30 minutes may be due to the adsorption of silver to the CdS thin film and a better photovoltaic performance due to the increase in photoconversion ability. A significant difference in absorption of all the samples was observed in the range between 537 and 800 nm, compared to the reference CdS sample. For smaller wavelengths, the absorption edges of the silver doped layers shifted to longer wavelengths than that of pure CdS, with a value of 504 nm. The band gap energy of thin films with Ag, decreased with respect to the CdS thin film. On the sequence of the samples measured, the band gap energies lowered to 2.25eV up until 45 min with respect to the reference material (CdS) of 2.46eV. After that time, the band gap energies rose again at 60 min and remained stable after that at 2.35eV. The decrease in band gap energy could be due to the doping of CdS with silver whereas the increase in band gap energy could be acquainted to etching due to surface saturation, leading to a higher concentration of precipitate.

Tiss et al. [36] synthesized silver doped In_2Se_3:Ag thin films by the spray pyrolysis method at 350^0C to analyze the corresponding physicochemical properties of the films. The films were reported to be semiconductor and the transport phenomena are assisted via small polaron hopping. The optical absorption showed opacity above the UV region and transmission above the visible and near-infrared region of the e.m. spectrum. The forbidden bandgap (E_g) increases with increasing Ag concentration. PL measurements reveal that the films exhibit seven emissions related to In_2S_3 defects and there is an improvement in peak intensity with Ag doping up to 4%, then decreased with higher Ag doping content. The PL intensity and crystallite size showed proportionality towards each other with respect to Ag content. Crystallization leads to higher recombination of the electron–hole pair that has improved the intensity of PL. The photovoltaic effect in Ag/In_2S_3(n)/Si(p)/Ag is confirmed by I–V characterization in dark and under illumination.

Thermal deposition of $(Se_{70}Te_{30})_{100-x}$ Ag_x($0.0 \leq x \leq 8.0$ at.%) semiconducting thin films which reveal a p-type behavior and shows interesting thermoelectric properties was reported by El-Denglawey et al [37]. As the Ag content in the structure of $Se_{70}Te_{30}$ increases, the Seebeck coefficient increases. The dark conductivity increases at 300 K, whereas a reduction in corresponding activation energy for dark, photo and thermal response is observed with the increase in the Ag content. The results indicate that these semiconducting thin films have remarkable potential as thermoelectric generators.

Abd-Elnaiem et al. [38] studied the effect of Ag content on the linear and nonlinear optical characteristics of thermal evaporated,100 nm thick, $Se_{90-x}Te_{10}Ag_x$ (x = 0, 2, 4, 6, and 8 at.%) thin films. Figure 3(a) and 3(b) shows the transmittance and reflectance spectra resp. at λ equal to 250–2500 nm, were used to assess various linear and nonlinear optical and electrical characteristics. Except for the optical band gap, the substitution of Se atoms by Ag reduces optical and electronic parameters such as absorption coefficient, extinction coefficient, optical conductivity, optical susceptibility, sheet resistance, and thermal emissivity. Figure 4(a) and 4(b) shows plots of $(\alpha h\nu)^2$ and $(\alpha h\nu)^{1/2}$ versus ($h\nu$) resp. for $Se_{90-x}Te_{10}Ag_x$ films. The extrapolating of the linear part to zero absorption in the $(\alpha h\nu)^{1/2}$-$h\nu$ curves gives the value of optical energy gap which increases from 1.65 to 1.89 eV as the Ag contents increase from 0 at.% to 8 at.% which means that the optoelectronic properties of the films could be controlled by the substitution of Se by Ag in the $Se_{90-x}Te_{10}Ag_x$ alloys. The change in the optical and electronic parameters with the substitution of Se with Ag may be due to the change in the amount of disorder, the density of defect states and polarizability in the systems and explained in terms of the cohesive energy and electronegativity (χ) differences between the elements used to create the $Se_{90-x}Te_{10}Ag_x$ glasses. These materials may be useful for optical memory systems due to their high absorption coefficients and compositional dependency on absorption.

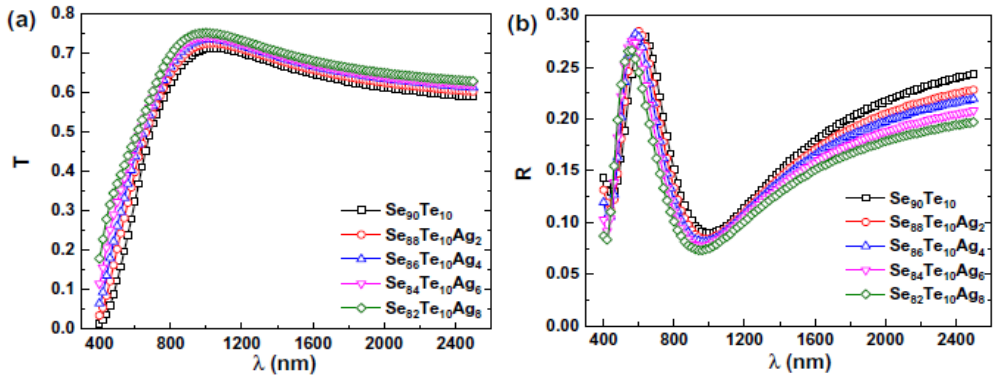

Figure 3: The optical (a) transmittance (T) and (b) reflectance (R) for the as-prepared $Se_{90-x}Te_{10}Ag_x$ films as functions of photon wavelength (λ).[38]

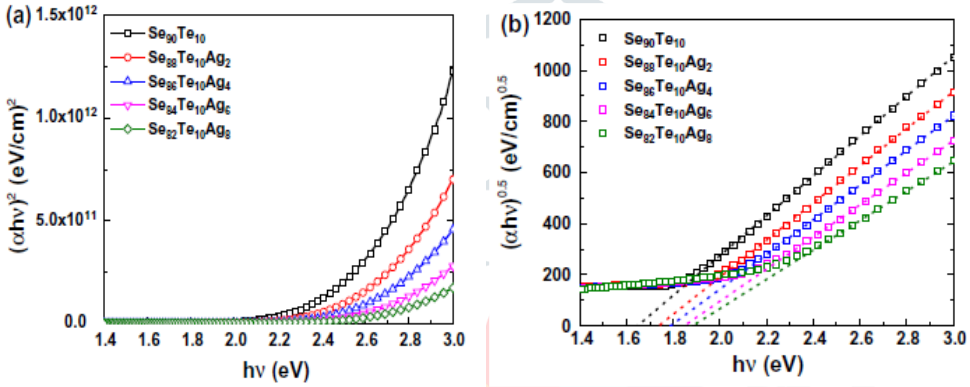

Figure 4: Plots of (a) $(\alpha h\nu)^2$, and (b) $(\alpha h\nu)^{1/2}$ versus $(h\nu)$ for $Se_{90-x}Te_{10}Ag_x$ films. (b) shows good linearity over a broad range of $h\nu$ which indicates that the dominant optical transition is allowed indirect type transition.[38]

B. Antimony doped chalcogenide glasses

Antimony doping changes the glassy network that affects the physical properties such as the atomic density, molar volume, molar mass, compactness, interatomic radius, packing density etc. Antimony substitution enhances the polarizability of the atom that affects the refractive index and other related optical parameters.

Mehra et al. [39] reported the effect of Sb impurity concentration on the steady state and transient photoconductivity of amorphous Se-Te films by exposing the material to white light. Photoconductivity is found to increase with the increase in Sb content and shows a square root dependence on intensity of light. The photosensitivity decreases with increasing Sb content. Non-exponential long-term photocurrent decays have been observed after ceasing the steady illumination. The results were explained on the basis of localized-localized recombination and it was found that Sb increases DOS near Fermi level by introducing $Sb^{(0,+)}$ ($D^{0,+}$) states. Temperature dependence (148–318 K) of dark conductivity and transient photoconductivity of thin films of a-$Ga_{20}Se_{80-x}Sb_x$ (where x = 0, 5, 10, 15 and 20) was reported by Khan et al. [40]. It has been found that at temperatures (287–318 K), the conduction is taking place in the band tails of localized states, while at temperatures (148–287 K), the conduction is due to variable range hopping which shows fair agreement with Mott's condition of variable range hopping. The transient photoconductivity observations made at different temperatures indicate non-exponential decay and recombination may be considered to take place through valence and conduction band.

Khan et al. [41] studied the optical band gap and optical constant for $Ga_{10}Te_{90-x}Sb_x$ (where x=5, 10, 20 and 30) thin films as a function of photon energy in the wave length region (720–1200 nm). The optical band gap (1.19 to 0.6 eV) and refractive index (15.16 to 2.23) decrease on incorporation of Sb in $Ga_{10}Te_{90-x}$ alloy. The change in the optical band gap may be due to the decrease in disorderedness of the materials and increase of the DOS. The dc conductivity of $Ga_{10}Te_{90-x}Sb_x$ thin films was also reported for the temperature range 308–368 K. DC conductivity (σ_{dc}) increases exponentially in the entire temperature range. The plot of ln σ verses 1000/T were straight line for all

the samples, indicating that conduction in these glassy alloys was through an activated process. The σ_{dc} decreases (1.49 to 0.12 $\Omega^{-1}cm^{-1}$ - decreases by one order of magnitudes on adding Sb), while the activation energy increases ($2.3x10^{-2}$ to $9.2\ x10^{-2}$ eV) on incorporating of Sb, which may be due to the alloying effect. The conduction might be due to thermally assisted charge carriers' movement in the band tail of the localized states.

D.C. conductivity measurements at high electric fields in vacuum evaporated thin films of amorphous $Se_{80}Te_{20}$, $Se_{75}Te_{20}Ge_5$ and $Se_{75}Te_{20}Sb_5$ systems have been reported by Singh et al [42]. I-V characteristics at various fixed temperatures shows ohmic behaviour at low electric fields and non ohmic behavior at high electric fields (10^4 V/cm). The density of defect states (DOS) near Fermi level is calculated using the theory of SCLC which was observed in all the glassy samples. An increase in DOS is observed for Sb whereas a decrease is observed for Ge as compared to a-$Se_{80}Te_{20}$ glassy system. Addition of Ge leads to the formation of Ge-Se tetrahedral units on the expense of Se-Te mixed rings. Fewer defects are expected to be introduced since tetrahedral structure has less flexibility of structural change as compared to Se-Te mixed rings. On the other hand, introduction of Sb does not produce tetrahedral structure but cross-links with Se-Te chains and also defect density further increase due to difference of electronegativity of Sb with Se and Te.

Dahshan et al. [43] reported the effect of replacement of Se by Sb on the steady state and the transient photoconductivity in vacuum evaporated amorphous thin films of $As_{30}Se_{70-x}Sb_x$(x = 2.5, 5, 7.5, 10, 12.5, 15 and 17.5 at.%). The composition dependence of the steady state photoconductivity at room temperature shows that the photoconductivity increases while the photosensitivity decreases with the increase in antimony content. The transient photoconductivity shows that the lifetime of the carrier decreases with increasing the light intensity and further suggested that the photoconductivity mechanism was controlled by the transition trapping processes. Replacement of Se by Sb results in a monotonic decrease in the band gap of $As_{30}Se_{70-x}Sb_x$ thin films and explained on the basis of the chemical bond approach. In addition to the optical and structural behaviour, Sb doping is much more useful for controlling the morphology of polycrystalline CG materials. Crystal aggregation with cross-linked grain coalescence was observed with doping Sb. However, with further Sb addition, those crystallites were broken down to form nanocrystalline particles with a significant influence on the alteration of optical statistics [44].

Compositional dependence of the optical and physical properties of as-deposited amorphous $Sb_xGe_{25-x}Se_{75}$ films (x = 0, 5, 10, 15 and 20 at. %), prepared by thermal evaporation, have been studied by Shaaban et al [45]. The refractive index, n, and film thickness, d, have been determined from the upper and lower envelopes of the transmission spectra, measured at normal incidence, in the spectral range from 400 to 2500 nm. The refractive index of the $Sb_xGe_{25-x}Se_{75}$ samples increases with increasing x, over the entire spectral range, which was related to the increased polarizability of the larger Sb atomic radius 1.38 Å compared with the Ge atomic radius 1.22 Å. Also, optical gap was found to decrease with increasing Sb content in $Sb_xGe_{25-x}Se_{75}$ glasses. M. Ali et al [46] investigated the effect Sb doping on physical properties of CdSe film. The electrical conductivity of the films was carried out with the help of impedance analyzer, which have been increased up to 1% on Sb doping. The transmission have been reduced up to 18% with the increase in Sb doping and shifted toward lower wavelengths. The incorporation of Sb results in structural changes such as a decrease in grain size that causes discrimination in electron diffusion. This results in an increase in conductivity and change in optical entities, such as the decrease in optical band energy and an increase in absorption that makes it more suitable for solar cell applications.

The influence of Sb addition on the electrical properties of $Se_{80-x}Te_{20}Sb_x$ (x=0, 6, 12) glasses was reported by Deepika et al [47]. Figure 5 shows that DC electrical conductivity decreases with increase in Sb concentration upto 6 at.% and on further addition of Sb upto 12 at.%, conductivity increases significantly. Glasses containing Se in higher atomic weight percentage mostly contains about 40% of Se atoms in ring structure and 60% of Se atoms are bonded as polymeric chains. When Te is added, Se_6Te_2 rings are formed at the expense of Se_8 rings. Thus, the structure of Se-Te is mixed network of Se_6Te_2rings, Se_8 rings and Se-Te copolymer chains. The rings are binded by strong covalent bonds while the chains have only Vander Wall bonds between them. The addition of Sb upto 6 at.% to Se–Te system causes its entry into the crosslink chains Se-Sb (214.20 kJ/mol) bonds of higher bond energy are formed replacing Te-Sb (205.8 kJ/mol) bonds of lower bond energy. This leads to a decrease in Se_8 rings which makes the system heavily cross linked. The steric hinderance increases which makes the system more rigid and results into decrease in dc electrical conductivity. On further increasing the concentration of Sb in Se-Te system, lower energy bonds (176.40 kJ/mol) of Sb-Sb bonds are favoured over Se-Sb bonds, which increases the Se_8 rings in the structure of Se-Te-Sb system. The increase in Se_8 rings makes the system more ordered by decreasing the degree of crosslinking and as a result increase in dc electrical conductivity is observed on addition 12 at.% of Sb to Se-Te system. I-V curves and the values of conduction activation energy indicate that conduction is mainly due to thermally assisted tunnelling of charge carriers. The density of localized states increases with increase in Sb content in the samples, which suggest that conduction in these glasses, was due to hopping into the localized states near Fermi level. The higher content of Sb in Se-Te system increases the electrical conductivity which makes it a potential candidate for application in electronic devices.

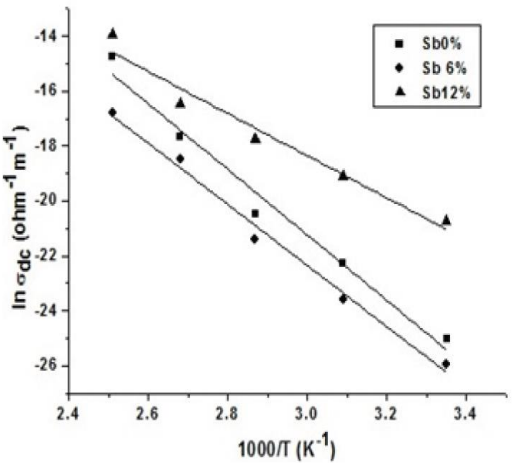

Figure 5: Temperature dependence of dc electrical conductivity for $Se_{80-x}Te_{20}Sb_x$ (x=0, 6, 12) glasses.[47]

Non-crystalline thin films of $Ge_{20}Te_{80-x}Sb_x$ (x = 0, 2, 4, 6, 10) systems were deposited on glass substrate using thermal evaporation technique [48]. The optical band gap shrinks with the addition of Sb due to the compositional change in the host network that in turn affects the bond angles and bond lengths. It was noticed that the Sb rich system, i.e., $Ge_{20}Te_{70}Sb_{10}$ sample showed a high value of the nonlinear refractive index, n_2(12.3 x 10^{-17} m^2 W^{-1}) and third order susceptibility, $x^{(3)}$ (2.43 x 10^{-12} esu), which was 1000 times higher than that of silica. The prepared Sb doped thin films on glass substrate may have a noble prospect in the application of nonlinear optical devices and might be used for a high-speed communication fiber. Pradhan et al. [49] studied the effect of Sb deposition onto As_2Se_3 film and its subsequent photo diffusion into As_2Se_3 matrix by 532 nm laser. The bilayer Sb/As_2Se_3 contains Sb as active, optical absorbing and diffusing layer and As_2Se_3 as barrier layer. It was observed that after photo diffusion, there is a shift of the optical absorption edge to higher photon energy. The absorption of high energy photons enhances the creation of homopolar bonds due to diffusion which increases the density of defect states. There is a decrease of E_g with the addition of Sb to As_2Se_3 and was explained on the basis of density of states and the increase in disorder in the system. The X-ray photoelectron spectroscopy measurements show the different bonding behaviour due to photo induced diffusion. This type of change is generally irreversible in nature which can be used for optical recording purpose.

Thin films having different thickness of Sb doped CdSe were deposited by thermal vacuum evaporation technique [50]. It was reported that Sb doped CdSbSe is a direct band gap material having value of 1.72 eV - 2.12 eV; the band gap decreases with increase of film thickness, hence the CdSbSe could be used in development of efficient photovoltaic application. The red shift of the absorption edge in Sb doped CdSe have been attributed to the charge-transfer transition between the Sb ion 5p-electrons and the CdSe conduction or valence band. Sb dopant may form a dopant energy level within the band gap of CdSe. The electronic transitions from the valence band to the dopant level or from the dopant level to the conduction band could effectively red shift the band edge adsorption threshold. The introduction of dopant (Sb) into CdSe causes transformation in the PL spectrum, due to generation of shallow levels in the band gap. The PL spectrum shows peaks in the infrared region, the bands at 825 and 970nm were due to a defect complex incorporating V_{Cd}^{2-} and Sb_{Cd}^{+} . Such a complex was revealed in studies of photo electric properties of CdSe (Sb).

Thin layers of CdSe doped with different concentrations of Sb prepared by the electron beam evaporation technique were investigated by S. Mathuri et al [51]. The transmittance of the CdSe films showed a reduced pattern with various amounts of Sb content and an enhancement in the E_g from 1.74 eV to 2.3 eV have also been observed. PL study showed two broad peaks at 605 nm and 743 nm, in which the former one corresponds to absorption edge and the latter corresponds to electron–hole pair recombination. The band's intensity varies with respect to the Sb content such that the 5% and 10% Sb doped film showed higher intensity with host CdSe matrix and then for 15% doped film showed decreased intensity and further increased for 20% Sb. These changes in PL intensity and the transition to a higher wavelength range could be due to the change in the crystalline size with doping Sb. Optical and structural characteristics of Sb doped $(Ge_{11.5}Se_{67.5}Te_{12.5})_{100-x}$ Sb_x glasses were analyzed by Mishra et al. [52]. Addition of Sb increases the absorption and extinction coefficient while E_g first increases and then decreases. Doping Sb with different concentrations expands the glass-forming ability, creates disorder, and modifies the glass matrix of the host system.

Hassanien et al. [53] prepared quaternary chalcogenide $Ge_{15-x}Sb_xSe_{35}Te_{50}$ ($0 \leq x \leq 15$ at.%) thin films by thermal evaporation process and reported that the E_g is due to the indirect electronic transitions; the values were found to decrease from 1.047 eV to 0.864 eV with the increase in Sb ratio. The band-tail width increases from 0.103 eV to

0.258 eV. The optical density, skin depth and extinction coefficient were found to increase with Sb-content. The compositional influence of Sb doping in $Ge_{15-x}Sb_xSe_{35}Te_{50}$ thin films enhances the absorbance capability by shifting the absorption edge towards a higher wavelength. This behaviour was primarily because of the solid metallic characteristic of Sb with a larger atomic volume than Ge, which increases the electronic polarizability, ultimately enhancing the loss of incident radiation through absorbance. However, Figure 6 shows that the Sb doping decreases the valence band potential, increasing the conduction band potential. Hence, this doping effect drives the corresponding valence levels closer to the Fermi level and decreases the transition width and transition energy of electrons, respectively.

Morphology, optical properties and electrical properties of the pure $In_{10}Se_{90}$ and Sb doped $(In_{10}Se_{90})_{100-x}Sb_x$ where x= (2, 5, 10) thin films deposited by thermal evaporation technique was reported by Sharma et al [54]. XRD shows that the incorporation of Sb does not change the characteristic peak (at 23.2°) as observed in pure $In_{10}Se_{90}$ indicating that no new phase is formed after the addition of Sb in $In_{10}Se_{90}$ however, with an increase in the concentration of Sb, the intensity of the existing phase is enhanced as the intensity of the peak is increased. I-V characteristics were linear for studied samples suggesting the ohmic nature exhibited by all alloys. TGA (Thermogravimetric analysis) and DSC (Differential Scanning Calorimetry) studies show that with increase in the concentration of Sb, the thermal stability of the films increases. The dielectric constant of the prepared films decreases with frequency and becomes constant at higher frequencies.

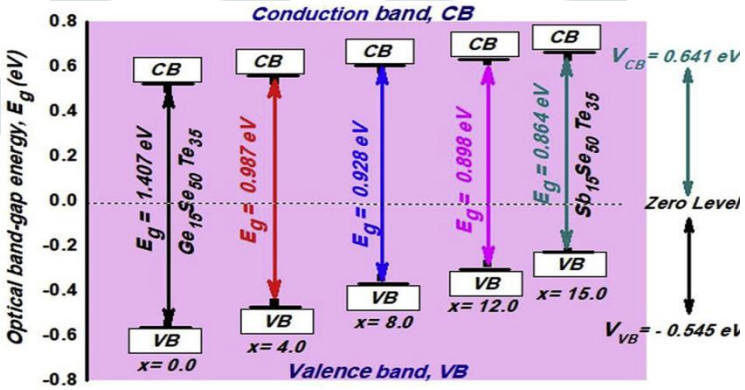

Figure 6. Conduction and valence band potentials of $Ge_{15-x}Sb_xSe_{35}Te_{50}$ compositions. [53]

The photosensitivity parameter (Σ- ratio σ_{ph} by σ_d where σ_{ph} and σ_d are photoconductivity and dark conductivity respectively), which is a crucial parameter for a specific material that elects the usage of the specimen material in the opto-electronics and activation energies of conduction for dark and light conditions(ΔE_{ph}) was calculated for thin-films of $Se_{80-x}Te_{20}Sb_x$ CGs obtained by thermal evaporation method [55]. It was found that both Σ and ΔE_{ph} were reduced with a rise in the concentration of Sb in the parent glass indicating that density of defect states was increased with an increase in the concentration of Sb in thin films of these glassy systems and explained by modified version of Kastner's model. The decrease in Σ could be attributed due to the appearance of charged defects $C_1^-$and C_3^+; the levels of such defects appear because of the occurrence of dangling bonds in the glassy network of the CGs. The chalcogens (i.e., Se and Te) belong to the identical group of the periodic table. Consequently, most of Te atoms are undoubtedly assorted in long polymeric chains of Se atoms. However, some of Te atoms behave like the ionized impurities because their electron affinity (1.97 eV) is lower than the atoms of Se (2.02 eV). Consequently, Te atoms play the role of the positively charged localized states. Correspondingly, the inclusion of Sb atoms having less electron affinity (1.07 eV) can persuade more positively charged localized states.

III. CONCLUSION

CG materials are among the most flexible and useful in current technology. The doping of suitable metals in the composition of CG glasses leads to desired structural and optical changes, making them suitable for several applications. Certain GeSbTe alloys are the basis of phase change memory technology (an alternative to conventional FLASH memory) and DVDs. Ag doped CGs are among the best-known solid electrolytes or 'fast ion conductors' and form the basis for a promising class of FLASH memory devices, 'conducting bridge' memory; they have applications in detection or sensing of radiation (a dosimeter), as programmable metallization cell devices, etc. There are still many more aspects of Ag and Sb based CGs that remains to be investigated towards their progress in technological applications.

REFERENCES

[1] Zakery, A. and S. R. Elliott, S. R. 2003.Optical properties and application of chalcogenide glasses - a review. J. Non- Cryst. Solids, 330:1–12.

[2] Tauc, J. 1970. The Optical Properties of Solids. Amsterdam, North-Holland; J. Tauc, J. 1968. Mater. Res. Bull., 3:37.

[3] Fadel, M., Sadeek, K. and Hegab, N. A. 2000. Effect of Sn content on the electrical and optical properties of $Ge_{1-x}Sn_xSe_3$ glasses. Vacuum, 57:307–317.

[4] Kumar, S. Singh, D. and Thangaraj, R.2013.Electronic structure and optical bandgap of silver photo diffused $Ge_2Sb_2Te_5$ thin film. Appl. Surf. Sci., 273:437–443.

[5] Kunda, N., Thakur, A., Singh, F. and Singh, A. P. 2020.Effect of ion irradiation on the optical properties of Ag-doped $Ge_2Sb_2Te_5$ (GST) thin films. Nucl. Instrum. Methods Phys. Res., Sect. B, 467:40–43.

[6]Tanaka, K. and Shimakawa, K. 2011. Amorphous Chalcogenide Semiconductors and Related Materials. Springer Publication, 63–84.

[7] Sharma, I., Kumar, P. and Tripathi, S. K. 2017. Physical and optical properties of bulk and thin films of a–Ge–Sb–Te lone-pair semiconductors. Phase Transitions, 90:653–671.

[8] Hassanien, A. S., Sharma, I. and Akl, A. A. 2020. Physical and optical properties of a-Ge-Sb-Se-Te bulk and film samples: Refractive index and its association with electronic polarizability of thermally evaporated a-$Ge_{15-x}Sb_xSe_{50}Te_{35}$ thin-films. J. Non-Cryst. Solids, 531:119853.

[9] Tanaka, K., Itoh, M., Yoshida, N. and Ohto, M. 1995. Photoelectric properties of Ag–As–S glasses. J. Appl. Phys., 78:3895.

[10] Kolomiets, B.T., Rukhlyadev, Y. V. and Shilo,V. P. 1971. J. of Non-Cryst. Solids, 5:389.

[11] Vautier, C. and Viger, C. 1971. J. of Non-Cryst. Solids, 23:287.

[12] Mitkova, M. 1997. Amorphous Insulators and Semiconductors. edited by Thorpe, M. F. and Mitkova, M. NATO ASI series, Kluwer Academic Publishers, page71.

[13] Kostyshin, M. T., Mikhailovskya, E. U. and Romanenko, P. F. 1966. Sov. Physics (Solid State), 8:45.

[14] Itoh, M. 1997. Electronic structures of Ag (Cu)–As–Se glasses. J. of Non-Cryst. Solids, 210: 178-186.

[15] Kawasaki, M., Kawamura, J., Nakamura, Y. and Aniya, M. 1999. Ionic conductivity of Ag_x $(GeSe_3)_{1-x}$ ($0 \leq x \leq 0.571$) glasses. Solid State Ionics, 123:259–269.

[16] Ribes, M., Bychkov, E. and Pradel, A. 2001.Ion transport in chalcogenide glasses: dynamics and structural studies. J. Optoelectron. Adv. Mater., 3:665–674.

[17] Belin, R., Taillades, G., Pradel, A. and Ribes, M. 2000. Ion dynamics in superionic chalcogenide glasses: complete conductivity spectra. Solid State Ionics, 136–137:1025–1029.

[18] Mytilineou, E., Petkova, T. and Skaperda, M. 2002. The effect of the addition of Ag and AgI on the density of defect states in a-Se. J. of Optoelectronics and Advanced Materials, 4(3):711 – 715.

[19] Singh, S. P., Kumar, S. and Kumar, A. 2004. Space charge limited conduction in $Se_{80-x}Te_{20}Ag_x$ thin films. Indian Journal of Pure & Applied Physics,42:615-620.

[20] Zha, C., Smith, A., Prasad, A., Wang, R., Madden, S. and Luther-Davies, B. 2007. Properties and structure of Ag-doped As_2Se_3 glasses. Journal of Nonlinear Optical Physics & Materials, 16(1):49-57. https://doi.org/10.1142/S0218863507003524.

[21] Mainika, Sharma, P., Katyal, S. C. and Thakur, N. 2009. A Study of Impurities (Ag, Bi & Ge) on the optical properties of Se-Te thin films. J. of Non-oxide Glasses, 1(2):90-95.

[22] Swanepoel, R. 1983. J. Phys. E: Sci. Instrum., 16:1214; Swanepoel, R. 1985. Determining refractive index and thickness of thin films from wavelength measurements only. J. Opt. Soc. Am. A, 2(8):1339–1343.

[23] Sanderson, R. T. 1971. Inorganic Chemistry. Affiated East-West Press PUT, New Delhi.

[24] Mulliken, R. S. 1934. A New Electroaffinity Scale; Together with Data on Valence States and on Valence Ionization Potentials and Electron Affinities. J. Chem. Phys., 2**:**78. https://doi.org/10.1063/1.1749394.

[25] Cui, S., Coq, D. L., Boussard-Pl´edel, C. and Bureau, B. 2015. Electrical and optical investigations in Te–Ge–Ag and Te–Ge–AgI chalcogenide glasses. J. Alloys Compd., 639:173-179. <10.1016/j.jallcom.2015.03.138>.

[26] Sakurai, M., Kakinuma, F., Matsubara, E. and Suzuki, K. 2002. Partial structure analysis of amorphous Ge15Te80M5 (M= Cu, Ag and In). J. Non-Cryst. Solids, 312:585-588.

[27] Messaddeq, S. H., Boily, O., Santagneli, S. H., El-Amraoui, M. and Messaddeq, Y. 2016. As_4S_4 role on the photoinduced birefringence of silver-doped chalcogenide thin films. Opt. Mater. Express, 6(5)**:**1451-1463. https://doi.org/10.1364/OME.6.001451.

[28] Ilcheva, V., Petkov, P., Petkova, T. and Boev, V. Silver containing chalcogenide glasses and their applications, presented at the Innovation Week on Renewable Energy Systems, Patras, Greece, 1–12 July 2012.

[29] Chen, Y., Min, J., Wang, Q. and Li, S. 2016. Metal sulfide precursor aqueous solutions for fabrication of Ag-doped $Zn_xCd_{1-x}S$ quantum dots thin films. J. Lumin., 180:258–263. https://doi.org/10.1016/j.jlumin.2016.08.035.

[30] Singh, P., Sharma, P., Sharma, V. and Thakur, A. 2017. Linear and nonlinear optical properties of Ag-doped $Ge_2Sb_2Te_5$ thin films estimated by single transmission spectra. Semicond. Sci. Tech., 32:045015. https://doi.org/10.1088/1361-6641/aa5ee0.

[31] Kumar, A., Kumar, D., Tripathi, S.K., Shukla, R.K. and Kumar, A. 2017. Role of Ag additives on light-induced metastable defects in a Se–In glassy system. J. of Taibah University for Science, 11(6): 1289-1295. DOI: 10.1016/j.jtusci.2017.05.003.

[32] Elliott, S.R. and Shimakawa, K. 1990. Model for bond-breaking mechanisms in amorphous arsenic chalcogenides leading to light-induced electron-spin resonance. Phys. Rev. B., 42:9766–9770; Shimakawa, K., Inami, S., Kato, T. and Elliot, S.R. 1992. Origin of photoinduced metastable defects in amorphous chalcogenides", Phys. Rev. B, 46:10062–10069.

[33] Yakoubi, A., Mrad, M., Chaabane, T. B., Rinnert, H., Balan, L., Medjahdi, G. and Schneider, R. 2018. Aqueous synthesis of highly fluorescent and color-tunable Ag^{+}-doped $Cd_xZn_{1-x}S$ quantum dots. J. Alloys Compd., 764(5):591-598. https://doi.org/10.1016/j.jallcom.2018.06.118.

[34] Viswanathan, A. and Thomas, S. 2019. Tunable linear and nonlinear optical properties of Ge-Se-Sb chalcogenide glass with solute concentration and with silver doping, J. Alloys Compd., 798:424–43. https://doi.org/10.1016/j.jallcom.2019.05.261.

[35] Corral-Guerrero, R. A., Ochoa-Landín, R., Apolinar-Iribe, A., de Leon, A. and Castillo, S. J. 2021. Silver doped cadmium sulfide thin films on a PET flexible substrate. Chalcogenide Letters, 18(6):351 – 355.

[36] Tiss, B., Moualhi, Y., Bouguila, N., Erouel, M., Kraini, M., ALaya, S., Aouida, S.,Vazquez, C. V., Moura, C. and Cunha, L. 2021. Influence of silver doping on physical properties of sprayed In_2S_3 films for solar cells application. J. Mater. Sci. Mat. Elect., 32:4568–4580. https://doi.org/10.1007/s10854-020-05198-2.

[37] El-Denglawey, A., Sharma, P., Kumar, P., Sharma, E., Sati, D.C., Aly, K. A. and Dahshan, A. 2021. Dark, photo and thermally driven conductivity of Ag-mixed $Se_{70}Te_{30}$ semiconducting thin films for thermoelectric applications. J. Mater. Sci: Mater. Electron., 32:25074–25083. https://doi.org/10.1007/s10854-021-06963-7.

[38] Abd‐Elnaiem, A. M., Abdelraheem , A. M. , Abdel‐Rahim, M. A. and Moustafa, S. 2022. Substituting Silver for Tellurium in Selenium–Tellurium Thin Films for Improving the Optical Characteristics. J. Inorg. Organomet. Polym., 32:2009–2021. https://doi.org/10.1007/s10904-022-02250-y.

[39] Mehra, R. M., Kaur, G. and Mathur, P. C. 1993. Effect of antimony impurity on photoconduction in thin films of Se-Te system. Solid State Commun., 85(1):29-31.

[40] Khan, Z. H., Zulfequar, M., Malik, M. M. and Husain, M. 1998. Effect of Sb on Transport Properties of Thin Films of a-$Ga_{20}Se_{80-x}Sb_x$. Jpn. J. Appl. Phys., 37:23-28. https://doi.org/10.1143/JJAP.37.23.

[41] Khan, S. A., Zulfequar, M., Khan, Z. H., Ilyas, M. and Husain, M. 2002. Optical and electrical properties of glassy $Ga_{10}Te_{90-x}Sb_x$ alloys. Optical Materials, 20(3):189-196, https://doi.org/10.1016/S0925-3467(02)00054-X.

[42] Singh, S. P., Kumar, S. and Kumar, A. 2004. Effect of some metallic impurities on the density of localized states in a-$Se_{80}Te_{20}$ thin films. Vacuum, 75:313-320.

[43] Dahshan, A., Amer, H. H., Moharam, A. H. and Othman, A. A. 2006. Photoconductivity of amorphous As–Se–Sb thin films. Thin Solid Films, 513(1-2):369-373. https://doi.org/10.1016/j.tsf.2006.01.062.

[44] Patil, N. S., Sargar, A. M., Mane, S. R. and Bhosale, P. N. 2008. Growth mechanism and characterisation of chemically grown Sb doped Bi2Se3 thin films. Appl. Surf. Sci., 254(16):5261–5265. https://doi.org/10.1016/j.apsusc.2008.02.084.

[45] Shaaban, E. R., Kaid, M. A., Moustafa, E. S. and Adel, A. 2008. Effect of compositional variations on the optical properties of Sb–Ge–Se thin films. J. Phys. D: Appl. Phys., 41(12):125301, https://doi.org/10.1088/0022-3727/41/12/125301.

[46] Ali, M., Syed, W. A. A. , Zubair, M., Shah, N. A. and Mehmood, A. 2013. Physical properties of Sb-doped CdSe thin films by thermal evaporation method. Appl. Surf. Sci., 284:482–488. https://doi.org/10.1016/j.apsusc.2013.07.122.

[47] Deepika and Hukum, S. 2016. Role of Sb Substitution on Electrical Properties of Se-Te Glasses. Indian Journal of Science and Technology, 9(48):1-8. DOI:10.17485/ijst/2016/v9i48/105687.

[48] Kumar, P., Kaur, J., Tripathi, S. K. and Sharma, I. 2017. Effect of antimony (Sb) addition on the linear and nonlinear optical properties of amorphous Ge–Te–Sb thin films. Indian J. Phys., 91(6):1503–1511.

[49] Pradhan, P., Naik, R., Das, N. and Panda, A. K. 2017. Laser induced optical properties change by photo diffusion of Sb into As_2Se_3 chalcogenide thin films. Optics & Laser Technology, 96:158-165.

[50] Tayade, D. A., Toda, Y. R. and Gujarathi, D. N. 2018. Surface morphological and Optical Properties of antimony doped CdSe Thin Films by Thermal Vacuum Evaporation Technique. Int. J. Sci. & Eng. Res., 9(12):1878-1890.

[51] Mathuri, S., Ramamurthi, K. and Babu, R. R. 2018. Effect of Sb incorporation on the structural, optical, morphological and electrical properties of CdSe thin films deposited by electron beam evaporation technique. Thin Solid Films, 660:23–30.

[52] Mishra, S., Lohia, P. and Dwivedi, D. K. 2019. Structural and optical properties of $(Ge_{11.5}Se_{67.5}Te_{12.5})_{100-x}$ Sb_x ($0 \leq x \leq 30$) chalcogenide glasses: A material for IR devices. Infrared Phys. Technol., 100:109–116, DOI:10.1016/j.infrared.2019.05.001.

[53] Hassanien, A. S. and Sharma, I. 2019. Band-gap engineering, conduction and valence band positions of thermally evaporated amorphous Ge_{15-x} Sb_x Se_{50} Te_{35} thin films: Influences of Sb upon some optical characterizations and physical parameters. J. Alloys Compd., 798:750-763, https://doi.org/10.1016/j.jallcom.2019.05.252.

[54] Sharma, M.D. and Goyal, N. 2020. Optical and electrical studies of doped In-Se system for phase-change memory applications. Chalcogenide Letters, 17(6): 321 – 328.

[55] Saraswat, S., Tomar, V.K, Deolia, V. K, Kumar, D. and Dahshan, A. 2021. Photosensitivity of semiconducting SeTeSb glasses. IOP Conf. Ser.: Mater. Sci. Eng., 1116(1): 012040, doi:10.1088/1757-899X/1116/1/012040.